PACS numbers: 42.55.Lt; 42.60.Lh; 52.80.-s
DOI: 10.1070/QE2010v040n01ABEH014165

Kinetics of processes and energy distribution in an electric discharge upon pumping a XeCl laser

Yu.I. Bychkov, S.A. Yampolskaya, A.G. Yastremsky

Abstract. **Radiation energies and efficiencies of the XeCl laser are calculated for different pump regimes in a broad range of variations in the initial parameters [pump energy of 50 – 350 J L^{-1}, pulse duration of 30 – 150 ns, initial concentration of HCl molecules of (0.7 – 2.5) $\times 10^{17}$ cm^{-3}]. The sequence of kinetic processes during which the pump energy is converted into induced radiation and heat is determined. It is shown that when 80 % – 90 % of the initial HCl concentration is used per pulse, the optimal ratio between the radiation energy and the laser efficiency is provided. In these regimes, about 50 % of the pump energy is spent on production of excimer molecules in the entire range of the experimental parameters and for one HCl molecule 10 ± 1.5 eV is spent.**

Keywords: *XeCl laser, simulation, kinetic processes, optimisation.*

1. Introduction

Interest in the XeCl laser as a high-power UV source appeared in 1980s. For the last 15 years, hundreds of papers have been published in this field. Different schemes of the active medium excitation, geometrical dimensions of the gas volume and the ratios of the initial pump parameters have been suggested. By now, lasing at the pulse durations from tens to several hundreds of nanoseconds with the specific radiation pulse energy in the pulse up to ~ 8 J L^{-1} and output power up to ~ 10 MW has been obtained in the electric discharge XeCl laser.

Table 1 lists the data of the experimental papers in which high characteristics of laser radiation were obtained and presents a rather complete description of the pump regimes. The comparative analysis of the given data showed that despite the inhomogeneity of the discharge used for pumping, which is inevitable in the experiment and always complicates the interpretation of its results, we deal with a dependence of the laser efficiency and radiation pulse energy on the pump power and the pulse duration. The highest laser efficiency (4 % – 5 %) with the specific radiation energy 2 – 3 J L^{-1} was obtained at pulse durations of 20 – 100 ns and specific pump powers of ~ 0.5 MW cm^{-3}. At the ~ 50-ns pulse duration and the 2 – 10-MW cm^{-3} specific pump power, the regimes with a high specific radiation energy (up to 7 J L^{-1}) were achieved at a lower efficiency (1 % – 3%). In the regimes with a small excitation pulse duration (30 – 20 ns), it is necessary to increase the pump power. In this case, a larger output power (up to 10 MW) can be achieved at the laser efficiency of 2 % – 3 %.

The aim of this paper was, using the computer simulation, to determine the kinetic processes related to the energy losses in the plasma; to elucidate the possibility to decrease these losses; to establish the dependence of the radiation parameters on the initial pump parameters, namely, on the pump energy, excitation pulse duration, and the content of the halogen donor in the initial gas mixture; to find the initial excitations conditions under which the optimal ratio between the radiation energy and the laser efficiency can be realised.

2. Zero-dimensional model of the XeCl laser

The XeCl-laser model with a homogeneous pump discharge (zero-dimensional) includes a system of equations describing the temporal changes in the concentration of plasma particles, the Boltzmann equation for the electron energy distribution function (EEDF), equations for electric pump circuits, and the radiation transfer equation in the resonator.

The model took into account the concentrations of electrons, negative ions Cl^-, positive atomic ions Ne^+, Xe^+, H^+, Cl^+, and molecular ions Ne_2^+, $NeXe^+$, Xe_2^+. In addition, we derived generalised equations for excited states of the particles, each of them combining the group of real levels. For neon atoms, we took into account two levels: Ne(1) combining 3s levels, and Ne(2) combining other levels. The excitation energies of Ne(1) and Ne(2) levels are 16.6 and 18.3 eV, respectively. For xenon atoms, we took into account three electron-excited levels: Xe(1), Xe(2), Xe(3). The Xe(1) level has the excitation energy of 8.3 eV and combines two 6s levels. The Xe(2) level has the excitation energy of 9.4 eV and combines 6s$'$, 6p, and 6d levels. The Xe(3) level has the excitation energy of 9.9 eV and combines all other upper levels. For the HCl molecule, we took into account the electron excitation in the A state with the 5.5-eV energy and the level combining B and C states with the 9.3-eV energy.

To calculate correctly the influence of the dissipative attachment of electrons to the HCl molecules, we took into account the processes with the participation of HCl molecules at the ground ($\upsilon = 0$) and first three vibrational levels:

Yu.I. Bychkov, S.A. Yampol'skaya, A.G. Yastremskii Institute of High Current Electronics, Siberian Branch, Russian Academy of Sciences, prosp. Akademicheskii 2/3, 634055 Tomsk, Russia; e-mail: bychkov@lgl.hcei.tsc.ru

Received 9 June 2009
Kvantovaya Elektronika **40** (1) 28 – 34 (2010)
Translated by I.A. Ulitkin

Table 1. Data borrowed from some published papers.

Specific pump power P_p/MW cm^{-3}	Laser pulse duration Δt/ns	Specific pump energy E_p/J L^{-1}	Specific radiation energy E_{las}/J L^{-1}	$\eta = E_{las}/E_p$ (%)	Initial concentration N_0 of HCl molecules /10^{16} cm^{-3}	References
0.05	210	46	1.0	2.2	5.4	[1]
0.1	450	45	0.58	1.3	10.5	[2]
0.2	190	79	2.37	3.0	5.8	[3]
0.2	200	57	1.43	2.5	3.8	[4]
0.46	170	92	1.57	1.7	4.3	[5]
0.46	120	84	3.54	4.2	10.7	[6]
0.56	150	82	3.38	4.1	4.0	[7]
0.81	80	84	2.11	2.5	13.5	[8]
0.94	95	83	4.14	5.0	10.8	[9]
1.45	90	333	4.0	1.2	12.7	[10]
2.9	20	195	3.9	2.0	10.6	[11]
3.28	7	45	0.58	1.3	8.9	[12]
6.2	50	300	7.8	2.6	2.5	[13]
10.36	15	714	5.0	0.7	20.8	[14]

HCl($\upsilon = 1$), HCl($\upsilon = 2$), and HCl($\upsilon = 3$) with the energies 0.36, 0.7, and 1 eV, respectively. The model also included the ground state X of the excimer XeCl molecule and five levels with electronic and vibrational excitation: the XeCl(B_0) state with the zero vibrational excitation and 4.025-eV energy; the XeCl(B) state with the 4.064-eV energy combining all the vibrational levels of the B state; the XeCl(C_0) state with the zero vibrational excitation and the 4.015-eV energy; the XeCl(C) state with the 4.045-eV energy combining all other vibrational levels of the C state; and the XeCl** state with the 8-eV energy combining upper excited levels. Simulation was performed in a broad range of variations in the initial parameters of the XeCl laser by neglecting fitting coefficients.

The Boltzmann equation for the EEDF was solved within the local field approximation taking into account elastic and inelastic collisions of electrons with atoms and molecules of the medium, impacts of the second kind, electron – electron and electron – ion collisions.

We simulated the processes in the resonator by using the one-dimensional transfer equation in which radiation in the resonator represents a sum of fluxes propagating in opposite directions between the plane mirrors.

The results of calculations are the time dependences of the particle concentration, the rate of processes, the power spent in the processes as well as the time dependences of the currents in the circuit, the voltage across the plasma, and the output power. A more detailed model was discussed in paper [15].

3. Results of numerical experiments and their comparison with experimental results

Conclusions drawn in this paper are based on the results of simulation of three laser systems [13, 16, 17]. They differ in the excitation pulse duration, pump power, the ratio of the components of the gas medium. The operation regimes of these systems virtually overlap the range of working conditions in which generation of the electric-discharge XeCl laser is possible. The initial conditions and parameters of radiation for these three experimentally obtained regimes are presented in Table 2.

Figure 1 presents, for the pump regimes listed in Table 2, the calculated time dependences of the pump power and output power of the XeCl laser and the experimentally measured time dependence of the output power. A good agreement between the results of calculations and the experiment both in the radiation pulse shape and in absolute values of the energy and maximum output power is observed for all the three pump regimes.

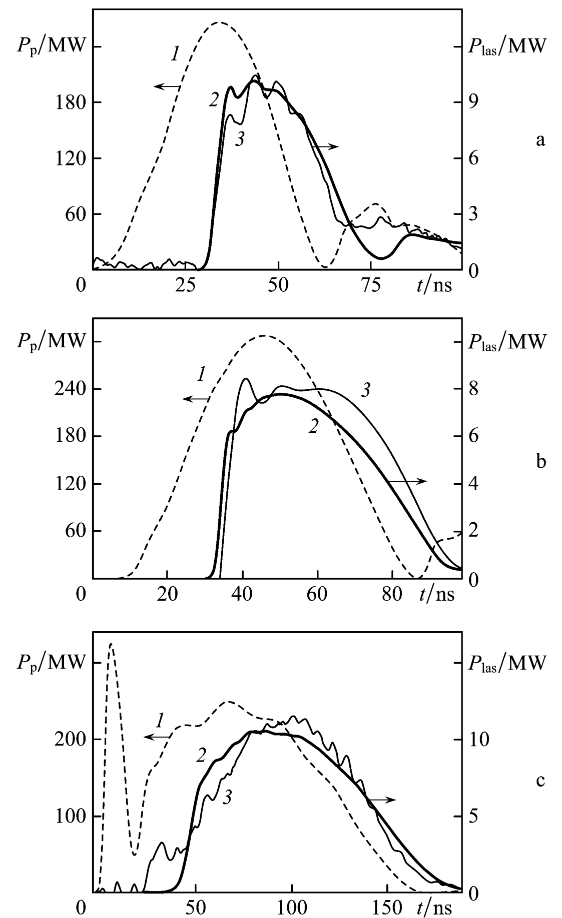

Figure 1. Calculated time dependences of the pump power (*1*), output power (*2*), and the output power measured in the experiment (*3*) for the regimes with the maximal laser energy obtained experimentally in papers [16] (a), [13] (b), and [17] (c) (initial parameters are listed in Table 2).

4. Kinetic processes in the XeCl-laser plasma

Consider in detail the kinetic processes in plasma for regime 2 (Table 2). This regime differs from typical operation regimes of XeCl lasers by a high gas pressure, a large partial pressure of HCl molecules, and a high pump power, which made it

Table 2. Initial conditions and radiation parameters obtained experimentally for operation regimes of the XeCl laser, which are analysed in this paper.

Regime	Δt/ns	Mixture composition Ne : Xe : HCl	p/atm	V/cm^3	P_p/MW cm^{-3}	W_p/J	W_{las}/J	η (%)	References
1	30	770 : 8 : 1.1	3.6	100	2.7	11	0.35	3.2	[13]
2	50	1000 : 5 : 1.7	6	50	6.2	17.5	0.38	2.2	[16]
3	150	2660 : 24 : 3	3.5	420	0.6	25	1	4	[17]

Notes: p is the mixture pressure; V is the active medium volume; W_p and W_{las} are the pump and laser radiation energies.

possible to obtain experimentally the specific radiation energy of ~ 7.6 J L^{-1} with the pulse FWHM of ~ 50 ns.

4.1 Processes of ionisation and attachment of electrons

Figure 2 shows the time dependences of the electron concentration, the total concentration of xenon at three excited levels, the concentration of HCl($v = 0$) molecules, and the total concentration of vibrationally excited HCl($v = 1, 2, 3$) molecules. Figure 3 presents the calculated frequencies of basic processes of electron production and annihilation: direct ionisation of xenon Xe($i = 1, 2, 3$) atoms, attachment of electrons to HCl($v = 0$) molecules, and the total attachment of electrons to HCl($v = 1, 2, 3$) molecules, as well as recombination of electrons with NeXe$^+$ ions. The rate of the processes is the number of acts proceeding per unit time per electron.

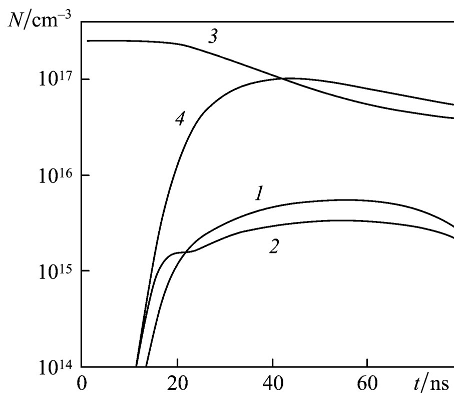

Figure 2. Time dependences of the concentrations of electrons (*1*), excited xenon atoms (*2*), HCl($v = 0$) (*3*) and HCl($v = 1, 2, 3$) (*4*) molecules in the discharge plasma.

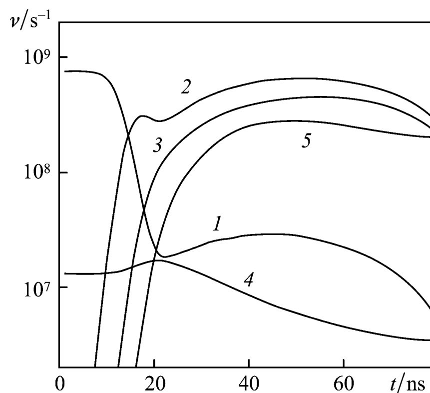

Figure 3. Rates of the main processes of electron production and annihilation: direct ionisation (*1*), step ionisation (*2*), recombination of electrons with NeXe$^+$ ions (*3*), attachment of electrons to HCl($v = 0$) molecules (*4*), and total attachment of electrons to HCl($v = 1, 2, 3$) molecules (*5*).

Note the typical features of time variations in the concentrations and rates of this regime. The development of the discharge within the first 8 ns is caused by the direct ionisation of xenon and attachment of electrons to HCl($v = 0$) molecules whose rates are equal to 0.75×10^9 and 1.3×10^7 s^{-1}, respectively. In this time interval, the field strength in the plasma is maximal, and the ionisation rate is much higher than the attachment rate. The concentration of electrons and excited xenon atoms increases with a higher rate, the total concentration of the excited xenon growing significantly faster than the electron concentration. At this stage, energy is accumulated on the metastable xenon levels, and the voltage across the discharge plasma is equal to the voltage across the capacitor and remains constant.

By the instant $t = 10$ ns, the electron concentration achieves $\sim 10^{13}$ cm^{-3}, while the total concentrations of excited xenon and HCl($v = 1, 2, 3$) molecules increase up to $\sim 10^{14}$ cm^{-3}. The growth of excited xenon and HCl($v = 1, 2, 3$) molecule concentrations results in a drastic increase in the rates of step ionisation and attachment of electrons to HCl($v = 1, 2, 3$) molecules. The total rate of the electron attachment to HCl($v = 1, 2, 3$) molecules is approximately 60 times greater than the attachment rate to the molecules in the ground HCl($v = 0$) state.

Within 10 – 20 ns, there occurs a drastic (by more than 30 times) decrease in the direct ionisation rate, caused by a decrease in the voltage across the plasma. Simultaneously, the rates of step ionisation and attachment of electrons to HCl($v = 1, 2, 3$) molecules increase. As a results of such changes, step ionisation and attachment of electrons to HCl($v = 1, 2, 3$) molecules become the basic processes of electron production and annihilation. These processes weakly depend on the field strength in the plasma, to a greater extent they depend on the concentrations of electrons, excited Xe($i = 1, 2, 3$) atoms, molecular NeXe$^+$ ions, and vibrationally excited HCl($v = 1, 2, 3$) molecules. The increase in the step ionisation rate decelerates the growth in the excited xenon concentration, and the concentration of electrons becomes higher than that of xenon. In step ionisation reactions, the excitation energy of xenon is transferred efficiently and more rapidly to xenon ions.

4.2 Recombination of charged particles

Electrons are annihilated both in reactions of dissociative electron attachment and dissociative recombination of electrons with molecular ions. For typical pump regimes of the XeCl laser, the recombination rate is higher than the attachment rate, and the difference in these rates increases with decreasing the initial concentration of HCl molecules in the gas mixture.

Note that in one recombination act the thermal energy losses make up only a small part of the xenon ionisation potential. During the recombination, an excited xenon atom Xe(3) with the 9.9-eV energy is produced, i.e. $\sim$ 1-eV energy in the recombination reaction is released as heat. In addition, the 1.2-eV energy loss occurs during the con-

version of the atomic Xe^+ ion into the molecular $NeXe^+$ ion. The re-combination reaction proves opposite to the step ionisation reaction. The energy of xenon excitation is multiply transferred from ion to excited states and vice versa. Due to ionisation and recombination acts, the ion and excited xenon concentrations remain constant, while the energy of the electron gas ($\sim$ 2.2 eV) is released as heat. At high rates, these thermal losses noticeably change of the energy balance in the plasma.

4.3 Production of excimer $XeCl^{**}$ and $XeCl(B_0)$ molecules

The active medium gain is proportional to the concentration of XeCl molecules in the B_0 state. The induced radiation cross section of these molecules is $\sim 6 \times 10^{16}$ cm^2. To obtain a sufficient gain, the concentration of $XeCl(B_0)$ molecules should be greater than 10^{14} cm^{-3}. The radiative lifetime of $XeCl(B_0)$ molecules is $\sim$ 11 ns, and the collisional quenching of excited molecules leads to a decrease in the lifetime down to $1-2$ ns. At this small lifetime of the upper laser level populations, a higher rate (more than 10^{23} cm^{-3} s^{-1}) of $XeCl(B_0)$ molecule production is required, which is a necessary condition both for developing and maintaining lasing.

Production of $XeCl(B_0)$ molecules is as follows. During the dissociation attachment of electrons to $HCl(\upsilon = 1, 2, 3)$ molecules accompanied by the production of a negative Cl^- ion and recombination of Cl^- and $NeXe^+$ ions, $XeCl^{**}$ molecules are produced at upper vibrational levels. Then, excited $XeCl^{**}$ molecules are relaxed via two intermediate $XeCl(B, C)$ levels to the $XeCl(B_0, C_0)$ levels with the zero vibrational excitation.

The recombination rate of $NeXe^+$ and Cl^- ions exceeds the electron attachment rate; therefore, $XeCl^{**}$ molecules are produced at the electron attachment rate. In turn, the electron attachment rate depends on the total concentration of $HCl(\upsilon = 1, 2, 3)$ molecules. The time dependence of the $HCl(\upsilon)$ concentration has a maximum (Fig. 2) after which the $HCl(\upsilon = 1, 2, 3)$ concentration starts decreasing, which is caused by a decrease in the concentration of $HCl(\upsilon = 0)$ molecules.

As a result, the production rate of excimer $XeCl(B_0)$ molecules is determined by the time dependence of the concentration of $HCl(\upsilon = 1, 2, 3)$ molecules. During the pump pulse, the electron attachment rate increases, achieves a maximum value, and then decreases. The stage of the attachment rate growth is caused by the increase in the concentration of $HCl(\upsilon = 1, 2, 3)$ molecules, and during this stage lasing develops. At the stage when the attachment rate is maximal, the output power is maximal. The stage of the attachment rate reduction is caused by the decrease in the concentration of $HCl(\upsilon = 0)$ and $HCl(\upsilon = 1, 2, 3)$ molecules. A noticeable 'burning-out' of $HCl(\upsilon = 0)$ molecules and a decrease in the concentration of $HCl(\upsilon = 1, 2, 3)$ molecules means that the resource of the gas mixture is exhausted.

Analysis of the kinetic processes in plasma allows one to determine in the general form the optimal ratios of the initial pump parameters such as the initial concentration N_0 of HCl molecules, the pump energy and power. The initial concentration N_0 predetermines the gas mixture resource, and the specific radiation energy can be only increased by increasing this concentration. The pump energy should correspond to the concentration N_0. When the pump energy is insufficient, the radiation energy decreases, while when it is overabundant, the laser efficiency decreases. The pump power should be high enough to provide the required electron attachment rate (i.e. the production rate of excited excimer molecules) for the given gas mixture.

5. Pump energy distribution of the XeCl-laser plasma

Figure 4 presents the general scheme of pump energy distribution and conversion in the plasma, constructed using the calculation data. We will single out two groups from the large number of kinetic processes. The first group includes processes consuming energy delivered to plasma and producing excimer $XeCl^{**}$ molecules. These processes are shemeatically illustrated in Fig. 4a. The thermal energy losses in the processes of this group occur in the collisional quenching of the excited particles, recombination of electrons with $NeXe^+$ ions, and during the conversion of the atomic Xe^+ ion to the molecular $NeXe^+$ ion. The second group includes kinetic processes of the excitation energy conversion of $XeCl^{**}$ into laser radiation (Fig. 4b).

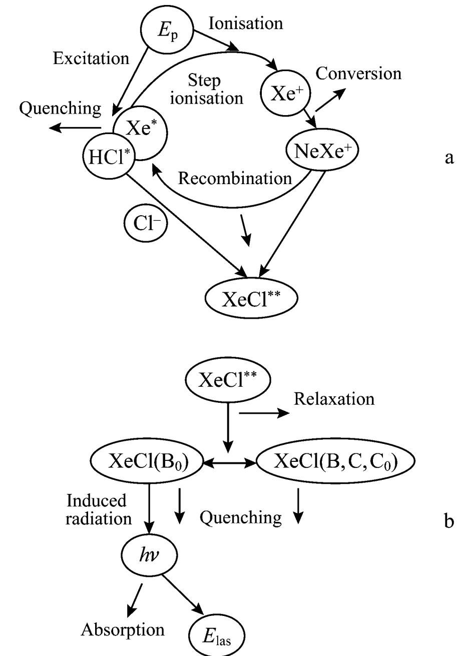

Figure 4. Diagram of the conversion of the pump energy in the discharge plasma (a) and the energy of the excimer $XeCl^{**}$ molecules into laser radiation (b).

The distribution of the calculated thermal losses (as a percentage of the pump energy E_p) for three regimes (Fig. 1) is given in Table 3. The total energy loss in other reactions not mentioned in the table does not exceed 5 %. Table 4 presents the consecutive pump energy conversion (as a percentage of E_p) into the energy of the excimer $XeCl^{**}$ molecules, $XeCl(B_0)$ molecules, induced photons produced in the resonator, and photons of the output radiation (laser efficiency).

It follows from the analysis of the data in Tables 3 and 4 that for all the regimes, the energy spent on the production of $XeCl^{**}$ molecules is equal to $\sim$ 50 % of the pump energy; the total energy of thermal losses is also $\sim$ 50 %. The first two regimes are characterised by higher pump powers and electron concentration. This lead to larger energy losses in

Table 3. Distribution of thermal energy losses per excitation pulse in main channels (as a percentage of E_p).

Regime	Channel				
	Quenching of $Xe(i = 1, 2, 3)$ $HCl(A, B, C, v = 1, 2, 3)$	Conversion and recombination of $(Xe^+ \to NeXe^+ + e)$	Relaxation of $(XeCl^{**} \to XeCl(B_0))$	Quenching of $XeCl(B, B_0, C, C_0)$	Absorption of induced photons in resonator
1	29	20.7	35	9.2	5.4
2	30	23.9	31	8.3	3.0
3	38	11.6	29	6.4	4.8

Table 4. Energy conversion per excitation pulse (as a percentage of E_p).

Regime	Channel			
	Production of $XeCl^{**}$	Production of $XeCl(B_0)$	Induced radiation in resonator	Laser radiation at output (efficiency)
1	50	12	8.6	3.2
2	46	12.5	5.6	2.2
3	45	14	9	4

the processes involving the charged particles (ion conversion and recombination) compared to the third regime. In the third regime, at a lower pump power and longer pulse duration, the energy losses in the quenching reaction of excited xenon and halogenide molecules increased significantly.

The energy losses in the second group of processes are determined by the relaxation of $XeCl^{**}$ molecules, the quenching of the excited $XeCl(B, B_0, C, C_0)$ molecules, and by photon absorption during the photodissociation of the molecular Xe_2^+ and $NeXe^+$ ions, photodetachment of electrons from the Cl^- ion, and photoionisation of excited $Xe(i = 1, 2, 3)$ atoms.

The excimer $XeCl^{**}$ molecules are produced mainly in ion–ion recombination reaction (up to 90 %), and only $\sim$ 10 % are produced in quenching reaction of the excited Xe^* xenon in collisions with the HCl molecules. The energy of the $NeXe^+$ ion equal to $\sim$ 11.2 eV is spent to excite one $XeCl^{**}$ molecule, and the excitation energy of the upper laser level $XeCl(B_0)$ is 4 eV. In this connection, $\sim$ 33 % of the pump energy is released as heat in the processes of relaxation of excimer molecules from the excited $XeCl^{**}$ levels to the upper laser level $XeCl(B_0)$.

In relaxation processes, four excited levels of excimer molecules – XeCl(B), $XeCl(B_0)$, XeCl(C), $XeCl(C_0)$ are taken into account. During the interaction with electrons or other particles, all these molecule are quenched. In addition, only the fourth part of $XeCl^{**}$ molecules undergoes a transition to the upper laser level $XeCl(B_0)$. As a result, lasing develops slowly and the laser pulse is delayed with respect to the pump pulse.

In the saturation regime, situations is improved: the concentration of $XeCl(B, B_0, C, C_0)$ molecules decreases and the losses during quenching are substantially reduced. However, the increase in the pump power leads to an increase in the energy losses during quenching processes. Thus, in regime 3, the pump power is the smallest; therefore, the energy losses in the quenching processes are 1.5 times lower than in other regimes.

It follows from the calculations that in different pump regimes, a high (up to 50 % of the pump energy) production efficiency of $XeCl^{**}$ molecules is retained, while the energy losses during the relaxation of $XeCl^{**}$, which are about 33 %, are independent of the pump conditions. Other losses depend on the gas mixture composition and the pump power. As the initial concentration of HCl is increased, it is necessary to increase the pump energy and power. In this case, the specific radiation energy and the energy losses increase, and the laser efficiency decreases.

6. Optimal pump regime

Figure 5 presents the calculated values of the specific radiation energy E_{las} and the laser efficiency η as a function of the pump energy. Other initial conditions corresponded to regime 2. The electrical excitation circuit represented a *LC* contour in which the inductance and the capacitance were equal to 3.3 nH and 144 nF, respectively. We performed calculations to optimise the laser with respect to the input energy. In these calculations, the pump energy was increased by increasing the charging voltage on the capacitor. Figure 5 demonstrates also the dependence of the con-centration of the unused halogen donor present in the gas medium after the end of the excitation pulse (as a percentage of the initial HCl concentration) on the pump energy.

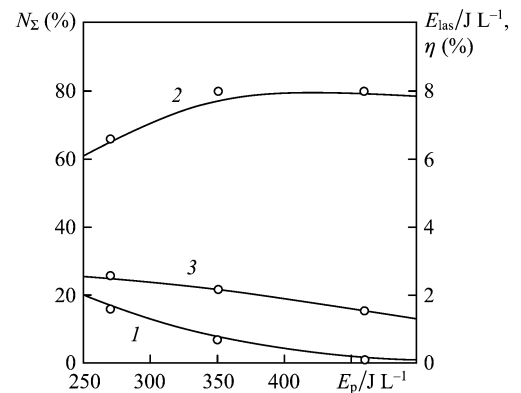

Figure 5. Calculated specific pump energy E_p as a function of the halogen donor concentration N_Σ residing in the medium after the pump pulse, taking into account all the excited levels including electronic (*1*), radiation energy (*2*), and laser efficiency (*3*). The initial parameters are borrowed from paper [13] (Table 2, regime 2).

As the pump energy is increased, the radiation energy increases, achieving a maximum value, and then slightly decreases. In this case, the concentration of the unused donor in the gas mixture decreases with increasing the pump energy. The energy increase is caused by an increase in the halogen burn-out, while the HCl molecules do not restore

during the action of the pump pulse. This implies that the initial HCl concentration determines the maximum possible radiation energy for the given gas mixture.

Simultaneously with the radiation energy increase, the laser efficiency decreases. The maximum specific radiation energy of 8 J L^{-1} was obtained with the 2 % efficiency for the specific pump energy of $\sim$ 400 J L^{-1}. In this case, the burn-out of the HCl molecules was 95 % of their initial concentration. The plotted dependences (Fig. 5) make it possible to select the optimal ratio of the pump energy, initial HCl concentration, and the laser efficiency. The specific pump energy, which corresponds to the HCl molecule burn-out in the concentration range from 80 % – 90 % of the initial concentration, can be considered optimal. The optimal specific pump energy for the data in Fig. 5 lies in the range from 250 to 300 J L^{-1}.

Figure 6 shows the pump energy E_p as a function of the fraction of its consumption in the kinetic processes of production of $XeCl^{**}$ molecules and in main processes accompanied by thermal losses. The energy losses in the reactions of electron – ion recombination and conversion of the atomic Xe^+ ion into the molecular $NeXe^+$ ion were combined because they depend on the concentration of charged particles, while the energy losses during quenching depend on the concentration of excited particles. The energy losses depending on the concentration of charged particles increase with increasing the pump energy. The energy losses due to the quenching of charged particles have an inverse dependence – they decrease with increasing the pump energy. These inverse dependences of the energy losses determine the maximum energy spent to produce $XeCl^{**}$ molecules.

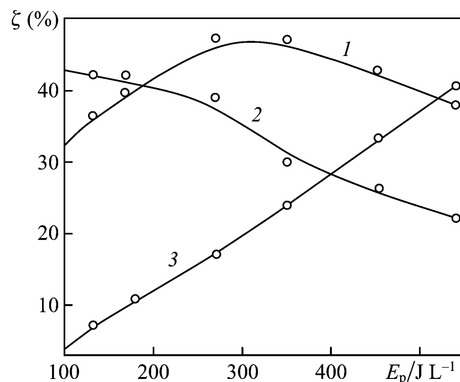

Figure 6. Calculated specific pump energy E_p as functions of the fraction of its consumption ζ during the $XeCl^{**}$ production (*1*), quenching of the excited states of Xe and HCl atoms (*2*), conversion and recombination (*3*). The initial parameters are the same as in Fig. 5.

At the $\sim$ 300-J L^{-1} specific pump energy, the maximal part (47 %) of the input energy is spent to produce excimer molecules (Fig. 6). With this pump energy, the burn-out of the HCl molecules was 86 % of their initial concentration. Therefore, the optimal pump energy is characterised by the fact that the maximum energy is spent on the production of $XeCl^{**}$ molecules in this case.

The energy distribution in the discharge plasma along the main channels depends on the electron concentration, which grows linearly with increasing the pump energy because for the given gas mixture, the voltage across plasma changes weakly and the pump energy increases with increasing the current. In the case of the low electron concentration, the energy is mainly lost during the quenching of the excited particles. As the electron concentration is increased, the energy transfer rates from the excited state system to ionic states increase due to step processes. Therefore, the thermal energy losses caused by the quenching of the excited states decrease, while the energy losses caused by the ion conversion and charge recombination, increase.

The excess pump energy exceeding the optimal one is released as heat in the processes with the participation of charged particles, which deteriorates the laser efficiency. At the pump energy lower than the optimal one, the potentials of the gas mixture remain unused.

7. Pump regimes with the optimal ratio of the initial HCl concentration and pump energy

Table 5 shows the calculation results of the regimes with the optimal ratio of the pump energy and the initial concentration of HCl. The pulse durations were in the range from 30 to 150 ns, and the specific pump energy was 78 – 350 J L^{-1}. The table lists the following data: specific pump and radiation energies, laser efficiency, initial concentration N_0 of HCl molecules, burn-out of halogenide molecules Δ_{HCl} (as a percentage of the concentration N_0), the energy ε_{HCl} spent to burn out one HCl molecule, which is equal to the ratio of the specific pump energy to the concentration of the used HCl molecules.

It follows from the calculations that the specific radiation energy decreases and the laser efficiency increases with decreasing the pump energy. The energy spent to burn out one HCl molecule weakly depends on the pump energy and is equal to 10 ± 1.5 eV in the entire range of the initial parameters under study. With good approximation, we can select, for evaluating calculations, the energy spent to burn-out one HCl molecule equal to 10 eV. This allows one to determine the optimal ratio between the specific pump energy and the initial concentration N_0 of HCl molecules in the gas mixture. The optimal specific pump energy is equal to $(0.9 - 0.8)\varepsilon_{HCl}N_0$.

The weak dependence of the energy spent on burning-out one HCl molecule on the pump energy is caused by the fact that in two main channels such as production of excimer molecules and quenching of excited states, large energy consumptions (up to 80 % of the pump energy) is determined by the concentration of HCl molecules. The energy consumption in the channel of the ion conversion and recombination, which is about 20 %, is independent of the HCl concentration but depends on the electron concentration. When the electron concentration is increased, the

Table 5. Calculation results for regimes with the optimal ratio of the concentration N_0 and the pump energy.

Δt/ns	E_p/J L^{-1}	E_{las}/J L^{-1}	η (%)	N_0 /10^{17} cm^{-3}	Δ_{HCl} (%)	ε_{HCl}/eV
35	175	5.8	3.3	1.6	83	8.2
35	138	4.43	3.2	1.18	86	8.6
30	132	4.4	3.3	0.8	81	12
	350	7.6	2.2	2.5	86	10
50	172	4.3	2.5	1.26	74	11.5
	142	2.2	1.6	0.85	70	10.8
	156	5.1	3.3	0.9	93	10.5
150	100	3.1	3.1	0.7	89	10
	78	2.9	3.7	0.7	71	9.5

energy consumption (up to $\sim 50\,\%$) spent on the production of the excimer molecules is retained. The other part of the pump energy is redistributed in other two channels, which leads to a decrease in the energy spent on quenching of the excited states and to an increase in the energy spent during ion conversion and recombination. This property is valid for all the regimes. Therefore, the pump energy per one HCl molecule remains virtually constant.

8. Conclusions

We have studied the kinetic processes in the discharge plasma of the XeCl laser. The radiation energies and the laser efficiencies have been calculated for different pump regimes in a wide range of variations in such initial parameters as the specific pump energy ($50-350$ J L^{-1}), the pulse duration ($30-150$ ns), the specific pump power ($0.6-6$ MW cm^{-3}), and the initial concentration of HCl molecules $[(0.7-2.5)\times 10^{17}$ $cm^{-3}]$.

We have determined the kinetic processes which affect the energy conversion and losses in the plasma. The dependences of the radiation parameters on the initial conditions have been elucidated. We have found the excitation conditions under which the optimal ratio between the radiation energy and the laser efficiency is realised.

Analysis of the results has allowed us to find out the following properties of the pump energy conversion into the energy of excited and ionised states, the energy of excited excimer molecules, the photon energy of induced radiation, and into the thermal loss energy:

(i) The production rate of excimer molecules (above 10^{23} cm^{-3} s^{-1}) required for generation in the XeCl laser is ensured by the step ionisation and attachment of electrons to the excited HCl($v = 1, 2, 3$) molecules. $XeCl^{**}$ molecules are produced at the rate of electron attachment and about 50 % of the pump energy is converted to the energy of $XeCl^{**}$ excitation in a wide range of the initial parameters.

(ii) The initial concentration N_0 of HCl molecules determines the potential resource of the gas mixture. For the optimal regimes, the energy spent on burning out one HCl molecule is equal to 10 eV in a wide range of the parameters. The optimal burn-out of the HCl molecules is $(0.8-0.9)N_0$. Then, the optimal ratio between the specific pump energy and the initial concentration N_0 has the form $E_{\rm p} = (0.9-0.8)\varepsilon_{\rm HCl}N_0$ and is retained at different pump conditions.

(iii) When the initial concentration N_0 is increased, the specific radiation energy increases, while the laser efficiency decreases, which is caused by the increase in the energy losses during the production of molecular ions and their recombination with electrons and during the collisional deexcitation of the excimer molecules.

(iv) The maximal laser efficiency (up to 4 %) is realised at low pump energies. In this case, the energy losses due to the collisional deexcitation of HCl($v = 1, 2, 3$) and Xe($i = 1, 2, 3$) increase, while they substantially decrease during the production of molecular ions and their recombination.

References

1. Baksht E.KH., Panchenko A.N., Tarasenko V.F. *Kvantovaya Elektron.*, **30**, 506 (2000) [*Quantum Electron.*, **30**, 506 (2000)].
2. Taylor R.S., Leopold K.E. *Rev. Sci. Instr.*, **65**, 3621 (1994).
3. Bernard N., Hofinann T., Fontaine B.B., Delaporte Ph., Sentis M., Forestier B. *Appl. Phys. B*, **62**, 431 (1996).
4. Van Goor F.A., Trentelman M., Timmermans J.C.M., Witteman W.J. *J. Appl. Phys.*, **75**, 621 (1994).
5. Bollanti S., Di Lazzaro P., Flora F., Giordano G., Letardi T., Schina G., Zheng C.E. *Appl. Phys. B*, **66**, 401 (1998).
6. Long W., Plummer M., Stappaerts E. *Appl. Phys. Lett.*, **43**, 8 (1983).
7. Fisher C., Kushner M., DeHart T., McDaniel J., Pert R., Ewing J. *Appl. Phys. Lett.*, **48**, 23 (1986).
8. Bychkov Yu.I., Vinnik M.L., Losev V.F. *Kvantovaya Elektron.*, **14**, 1582 (1987) [*Sov. J. Quantum Electron.*, **17**, 1002 (1987)].
9. Makarov M., Bonnet J., Pigach D. *Appl. Phys. B*, **66**, 417 (1998).
10. Hasama T., Miyazaki K., Yamada K., Sato T. *IEEE J. Quantum Electron.*, **25**, 1 (1989).
11. Panchenko Yu.N., Ivanov N.G., Losev V.F. *Kvantovaya Elektron.*, **35**, 816 (2005) [*Quantum Electron.*, **35**, 816 (2005)].
12. Komi T., Sugii M. *Rev. Sci. Instr.*, **65**, 7 (1994).
13. Riva R., Legentil M., Pasquires S., Puech V. *J. Phys. D: Appl. Phys.*, **28**, 856 (1995).
14. Steyer M., Voges H. *Appl. Phys. B*, **42**, 155 (1987).
15. Bychkov Yu.N., Makarov M.K., Yampolskaya S.A., Yastremsky A.G. *Opt. Atmos. Okean.*, **11**, 149 (1998) [*Atmos. Oceanic Opt.*, **11**, 132 (1998)].
16. Bychkov Yu.I., Losev V.F., Panchenko Yu.N., Yampolskaya S.A., Yastremsky A.G. *Proc. SPIE Int. Soc. Opt. Eng.*, **5483**, 60 (2003).
17. Bychkov Yu., Baksht E., Panchenko A., Tarasenko V., Yampolskaya S., Yastremsky A. *Proc. SPIE Int. Soc. Opt. Eng.*, **4047**, 99 (2002).